

Tuning the Carrier Injection Efficiency for Organic Light-Emitting Diodes<sup>†</sup>

E. W. Forsythe and M. A. Abkowitz\*

*Department of Chemistry and Center for Photoinduced Charge Transfer, University of Rochester, Rochester, New York 14627*

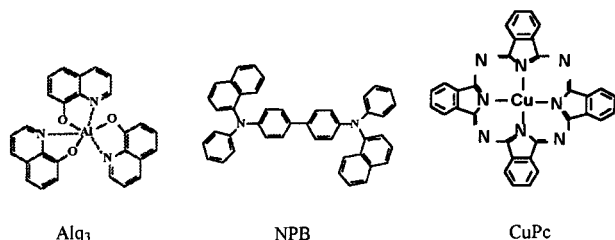
Yongli Gao

*Department of Physics and Astronomy, University of Rochester, Rochester, New York 14627**Received: October 26, 1999*

Organic light-emitting diodes based on tris-8-(hydroxyquinoline) aluminum and *N,N'*-diphenyl-*N,N'*-(2-naphthyl)-(1,1'-phenyl)-4,4'-diamine (NPB) ordinarily have an operating stability of less than 1000 h. Stability and efficiency are, however, dramatically enhanced by interposing a copper phthalocyanine (CuPc) layer between the indium tin oxide (ITO) anode and the NPB hole-transport layer. To specifically understand the origin of an interlayer-induced increase in light output, we have directly measured and analyzed the effective hole injection efficiency from ITO into NPB as a function of the CuPc interlayer thickness. Because NPB is trap free, a direct and self-consistent measure of the hole injection efficiency can be determined from the measured drift mobility and dark current at the same applied field. By this means, we have been able to demonstrate that the hole transport from the ITO anode to the NPB is injection-limited and that the hole injection efficiency is reduced progressively as the CuPc interlayer thickness is systematically increased in the range from 0 to 30 nm. In fact, the diminution of hole injection from ITO into NPB is already significant for a CuPc layer thickness of as little as 2 nm. The ITO anode used in the present study has a work function of 4.4 eV, as measured by ultraviolet photoemission spectroscopy. The increase in device efficiency induced by insertion of a CuPc layer is correlated with a decrease in hole injection efficiency. As a consequence, it must be attributed to an improved balance between hole and electron currents arriving at the recombination zone.

## Introduction

Organic-based light-emitting diodes have experienced remarkable advancement toward commercialization for flat-panel, high-brightness applications.<sup>1,2</sup> Devices based on tris-8-(hydroxyquinoline) aluminum and *N,N'*-diphenyl-*N,N'*-(2-naphthyl)-(1,1'-phenyl)-4,4'-diamine (NPB) ordinarily have an operating stability of less than 1000 h. The device stability is dramatically enhanced by interposing a copper phthalocyanine (CuPc) layer on the indium tin oxide (ITO) anode.<sup>3</sup>



It had been suggested by other workers that the CuPc layer lowers the drive voltage by reducing the effective barrier between the ITO substrate and the NPB hole-transporting layer.<sup>4,5</sup> Using ultraviolet photoemission spectroscopy, the ionization potential for thin, <2–3 nm layers of CuPc prepared under ultrahigh vacuum was determined to have a value of 5.0–4.8 eV.<sup>6,7</sup> In ref 7, the ITO work function is 4.3 eV.<sup>4</sup> On this

basis, the CuPc highest occupied molecular orbital (HOMO) might plausibly be expected to align energetically between the Fermi level of ITO and the estimated HOMO level of NPB, thereby enhancing the hole injection from the effective anode. Conversely, other researchers have shown that relatively thick, 15 nm CuPc layers will, in fact, reduce the rate of hole injection from the ITO anode, leading to a better balance with the electron current arriving from the cathode to the recombination zone.<sup>8</sup> In the latter work, it was also demonstrated that an excess of holes in the Alq<sub>3</sub> layer would create an unstable cation population, leading to a rapid degradation in device performance. It can therefore be inferred, on the basis of a comparison of these studies, that the physics underlying the operation of CuPc layers on OLED devices depends on layer thickness.

In the present study, we address this issue by employing a direct measure of the efficiency of hole injection from the ITO anode into a NPB hole-transporting layer as a function of the CuPc interlayer thickness through the entire range of interest. All features of device preparation and geometry are otherwise held constant. Measurements of OLED efficacy in units of candela per ampere have also been carried out. It is unambiguously demonstrated that the CuPc layer always acts as a barrier for carrier injection and that, in fact, the barrier increases for increasing CuPc thickness. Thus, it is the decreased hole injection leading to better charge balance in the recombination zone that, in all cases, underlies the observed increase in device efficiency of multilayer OLEDs. In the devices prepared using materials and substrates to be described in the following sections,

<sup>†</sup> Part of the special issue "Harvey Scher Festschrift".

we did not observe enhanced hole injection when thin CuPc interlayers were used.

The technique for the direct determination of the efficiency of carrier injection into trap-free transport media has been described in earlier publications<sup>9–11</sup> and is briefly summarized in the following.

The NPB organic layer is established to be trap-free by analysis of transport and Xerographic measurements. It has been established that transport occurs by hopping in a Gaussian manifold with a nominal width of 0.1 eV.<sup>12,13</sup> The hole injection behavior from the ITO anode into the NPB hole-transporting layer is characterized using conventional time-of-flight (TOF) and current density measured as a function of applied electric field ( $J$  vs  $E$ ), as described in the earlier studies.<sup>9–11</sup> A figure of merit for the injection efficiency is determined by first measuring the mobility ( $\mu$ ) from TOF and then calculating the trap-free space-charge-limited current density ( $J_{\text{TFSL}}$ ). If the contact under test (CUT) is ohmic and the bulk organic film is trap-free, then the current density when a voltage  $V$  appears across the device of thickness  $L$  is given by

$$J_{\text{TFSL}} = (9/8)\epsilon\epsilon_0\mu V^2/L^3 \quad (1)$$

where  $V$  is the applied voltage and  $\epsilon$  is the relative dielectric constant. If the current density supplied by a CUT is  $J_{\text{MEAS}}$ , then an operational figure of merit for the CUT supply efficiency is given by the quotient

$$J_{\text{MEAS}}/J_{\text{TFSL}} \quad (2)$$

Thus,  $J_{\text{MEAS}}/J_{\text{TFSL}} = 1$ , for the ohmic case, and  $J_{\text{MEAS}}/J_{\text{TFSL}} < 1$ , depending on the extent of the emission limitation.

## Experimental Section

Four TOF devices were prepared to test the hole injection efficiency of the ITO anode. The injection efficiency is measured as a function of the CuPc interlayer thickness between the ITO substrate and the NPB hole-transporting layer. The experimental apparatus is detailed in ref 8. The TOF samples were prepared simultaneously, and all layers were deposited without breaking vacuum. Prior to the organic deposition, the ITO substrates were cleaned by first being scrubbed with soap and deionized H<sub>2</sub>O (DH<sub>2</sub>O). The scrubbing was followed by two ultrasound rinses in DH<sub>2</sub>O, a toluene-vapor degreasing, and finally two additional ultrasound rinses with DH<sub>2</sub>O and isopropyl alcohol. The ITO substrates were O<sub>2</sub>-plasma etched using a Plasmatic Plasma Preen, leading to a final work function of 4.4 eV, as measured with ultraviolet photoemission spectroscopy.<sup>14,15</sup> It should be noted that the O<sub>2</sub>-plasma exposure time was sufficient to remove carbon residue from the ITO surface, but the final ITO work function did not increase, as reported previously.<sup>16,17</sup> If we increased the plasma exposure time, then we could, in fact, shift the ITO work function to 5.0 eV. However, the film appeared discolored in this case, possibly as a result of excessive substrate heating in this particular system. Immediately after cleaning, the ITO substrates were then loaded into a 46-cm-diameter evaporator with a source-to-substrate distance of 25 cm and a working base pressure of  $2 \times 10^{-6}$  Torr. The CuPc interlayers were evaporated at a rate of 2 Å/s to total thicknesses of 2.0, 15.0, and 30.0 nm. Deposition of the CuPc interlayer was followed, in each case, by the deposition of a 5.5-μm NPB layer, evaporated at a rate of 5 Å/s. Finally, a 13.0-nm Al metal cathode with an active area of 0.32 cm<sup>2</sup> was evaporated onto the device. The drift mobility of holes through each device was measured under small signal conditions with positive bias on

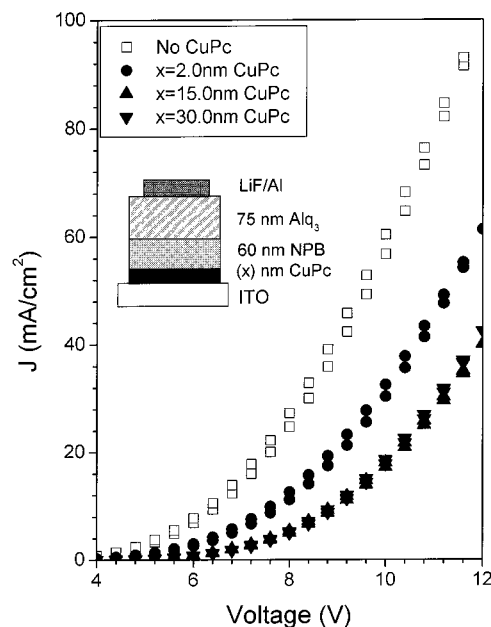


**Figure 1.** Current density as a function of applied voltage ( $J$  vs  $V$ ) for multilayer bipolar OLEDs as a function of CuPc thickness. A typical multilayer OLED is shown schematically in the inset. All measurements were carried out at room temperature in air.

the Al cathode using weak, 337-nm nitrogen laser pulses to create electron–hole pairs near the Al cathode. Al has a sufficiently high work function compared to the energy of the lowest unoccupied molecular orbital of NPB to ensure that the dark injection current is low compared to the TOF current; this condition was experimentally verified. The  $J$  vs  $E$  curves were then measured with a Keithley 2400 source measurement unit with a positive bias on the ITO substrate to measure the dark hole injection from the anode.

For the 2.0-, 15.0-, and 30.0-nm CuPc thicknesses, four multilayer organic light-emitting diodes (OLEDs) were prepared in a separate deposition. The ITO substrate was first cleaned as described above. The device structure consisted of ITO/CuPc ( $x$  nm)/NPB (60.0 nm)/Alq<sub>3</sub> (75.0 nm)/LiF (0.5 nm)/Al, where  $x = 0.0, 2.0, 15.0$ , and 30.0 nm. The current density versus voltage ( $J$  vs  $V$ ) characteristics were measured with a Keithley 2400 source measurement unit, and the electroluminescence (EL) emission was measured with a Photoresearch PR650 colorimeter. All measurements were conducted in air immediately following device fabrication.

## Results and Discussion

The  $J$  vs  $V$  characteristics for the four OLEDs as a function of CuPc thickness are plotted in Figure 1. A typical multilayer OLED is schematically illustrated in the inset of Figure 1. The drive voltage clearly increases as the CuPc thickness increases, even at the lowest coverage of 2.0 nm. Correspondingly, the EL efficacy in units of candelas per ampere first increases rapidly at the lowest CuPc coverage and then increases further for coverages of 2–15 nm. As the interlayer thickness is further increased, the efficacy of light emission slowly tapers off, as plotted in Figure 2. Our experimental results indicate that the decrease in efficacy in the range of 30 nm is associated with only a small decrease in the overall injection current density, which implies that, in this limit, other experimental factors such as optical factors play an increasingly important role.

Figure 3a is a representative family of TOF hole transients for one of the devices. These are plotted as a parametric function

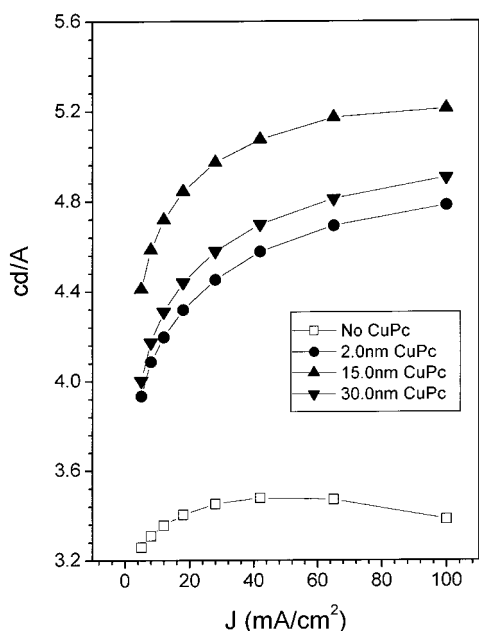


**Figure 2.** Efficacy of diode emission, in cd/A, as a function of current density and CuPc thickness. Shown are the results for multilayer bipolar OLEDs, as schematically illustrated in the inset of Figure 1.

of applied voltage from 50 to 150 V in 10 V increments across the approximately  $5.5\text{-}\mu\text{m}$ -thick TOF device with 30 nm of CuPc between the ITO substrate and the NPB transport layer. The TOF device structure is shown schematically in the inset of Figure 3b. The signals, which are all qualitatively similar, were each scaled by an arbitrary gain factor to clearly depict the dependence of the transit time on the voltage applied across the device. In each case, the initial drop from a well-defined plateau represents the transit time of the fastest carriers. The mobilities shown in Figure 3b for the entire set of devices represent, in each case, the average carrier arrival time at the collecting contact, and so, they were calculated using the time at which the TOF signal intensity fell to one-half the plateau amplitude.<sup>9</sup> Mobilities for the complete set of devices are represented in a semilog plot as a function of the square root of the applied electric field as a parametric family in CuPc thickness. The drift mobilities thus illustrated are the same within the experimental error of approximately 20% and show no systematic dependence on CuPc thickness. Furthermore, the TOF signals and corresponding drift mobilities for NPB are consistent with previous observations.<sup>12</sup> The presence of the CuPc layers, therefore, plays no measurable role in hole transport in these devices, and the inclusion of CuPc in the device fabrication process does not influence the transport properties of the NPB layer.

The  $J$  vs  $E$  curves for the same set of TOF devices are illustrated in Figure 4a, with the device shown schematically in the inset. Here, positive polarity steps are applied to the CuPc-overcoated ITO contact in the dark, and the hole dark current is recorded. In this relatively simple and well-characterized unipolar structure, we observe, at each fixed bias, a monotonic decrease in the current with increasing CuPc thickness. This process is clearly initiated at the thinnest coverage of 2.0 nm. The data have been replotted in Figure 4b on a log–log scale to accurately compare the measured current densities to the value of  $J_{\text{TFSL}}$  calculated using eq 1 and the measured mobilities from Figure 3b. Figure 4b clearly shows that the uncoated ITO anode, with its 4.4-eV work function, limits injection into an NPB hole-transporting layer. This result is also consistent with previous observations.<sup>18</sup> The present work demonstrates, by a self-

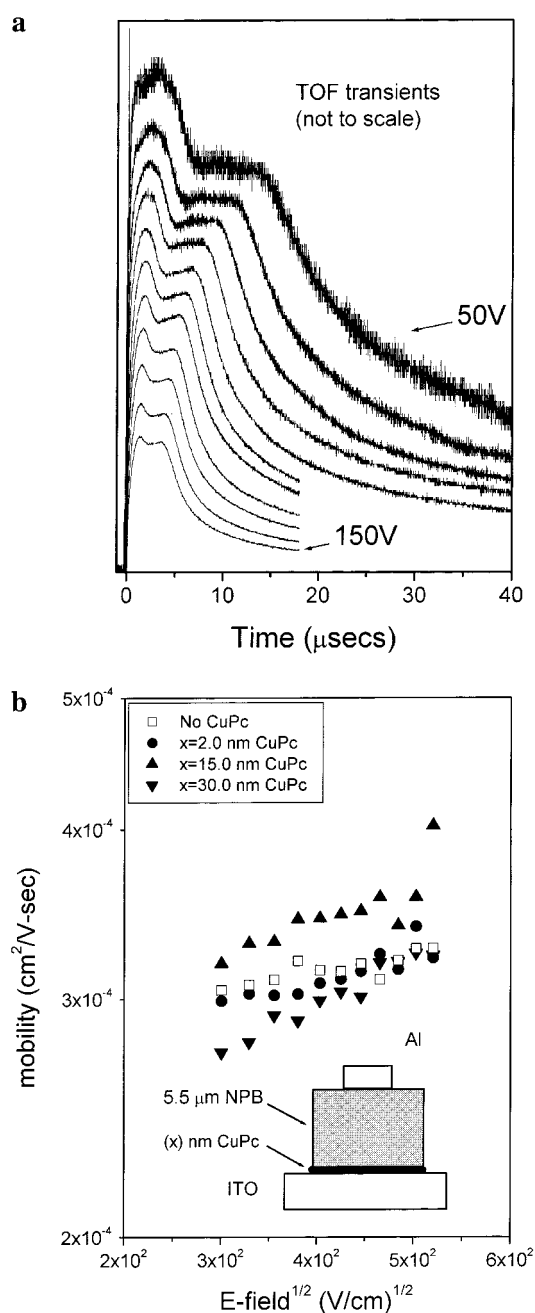


**Figure 3.** (a) TOF hole transients observed in a unipolar device consisting of an ITO anode overcoated with 30.0 nm of CuPc and  $5.5\text{-}\mu\text{m}$  of hole-transporting NPB with a 13.0-nm Al collecting electrode. Voltages applied to the device range from 50 to 150 V in 10 V increments. Respective transient amplitudes are not to scale. All measurements are carried out at room temperature in air. (b) Hole drift mobility in the unipolar TOF devices as a function of the square root of the applied electric field for various CuPc thicknesses. The carrier transit times through the devices are not affected by the CuPc interlayers. The inset is a schematic representation of the TOF devices.

consistent experimental procedure, that the addition of CuPc layers of increasing thickness, starting at 2 nm, monotonically reduces the efficiency of hole injection into the NPB transporting layer even further.

Figure 5 summarizes the results for the injection efficiency ratio,  $J_{\text{MEAS}}/J_{\text{TFSL}}$ , at  $1.81 \times 10^5$  V/cm and the device efficacy (in cd/A) at  $42\text{ mA/cm}^2$  as a function of the CuPc thickness (in nm). The efficacy of the OLED structure is improved by inclusion of CuPc layers in the 2–15 nm thickness range on the ITO substrate, whereas the injection efficiency for holes is

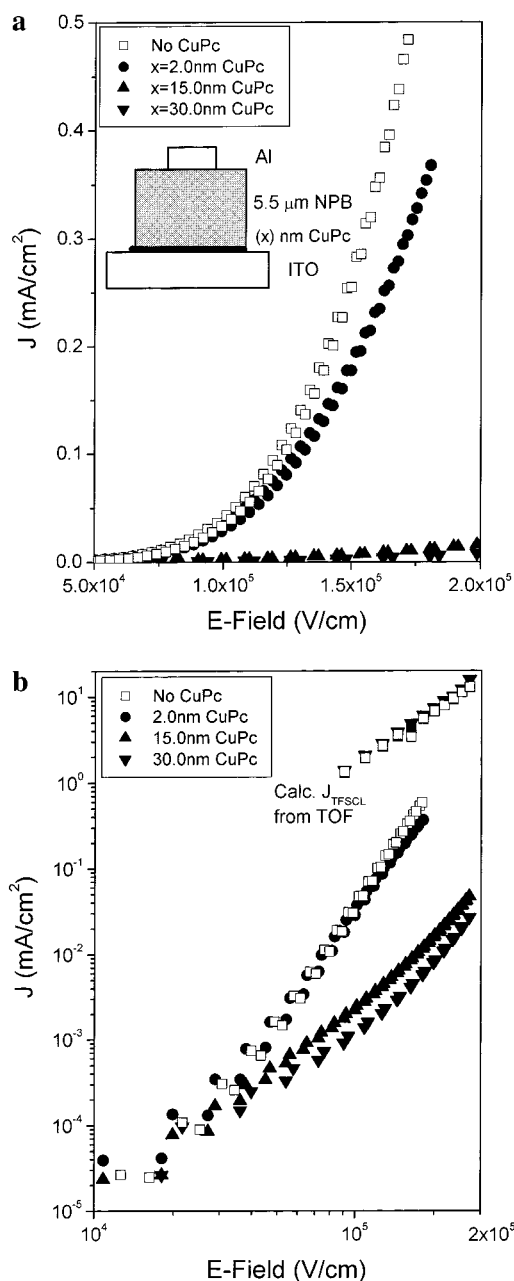


**Figure 4.** (a) Current density versus applied electric field for the same unipolar TOF devices as Figure 3 as a function of CuPc thickness. The TOF device schematic is repeated in the inset. (b) The data for Figure 4a replotted in log–log coordinates. In addition, the current density,  $J_{\text{TFSL}}$ , calculated from the field-dependent mobility is shown for the same devices. At a fixed field,  $J$  decreases monotonically with increasing CuPc thickness.

progressively diminished for similar CuPc layers on the ITO substrate in the TOF structures. These results taken together support the balanced current mechanism described in ref 8. Interestingly, the efficacy exhibits a shallow decrease from 15.0 to 30.0 nm. From the balanced carrier density argument, this observation may suggest an eventual transition, as the CuPc layer thickness is increased further, to nonoptimal hole supply at the recombination zone.

In the TOF structures, the CuPc layer and the ITO substrate can be thought of as together forming an emission-limited contact with an effective barrier that progressively increases with increasing CuPc thickness. The effective barrier can, in principle, be affected by CuPc energetics and microstructural and spatial parameters and may be sensitive to preparatory conditions. In

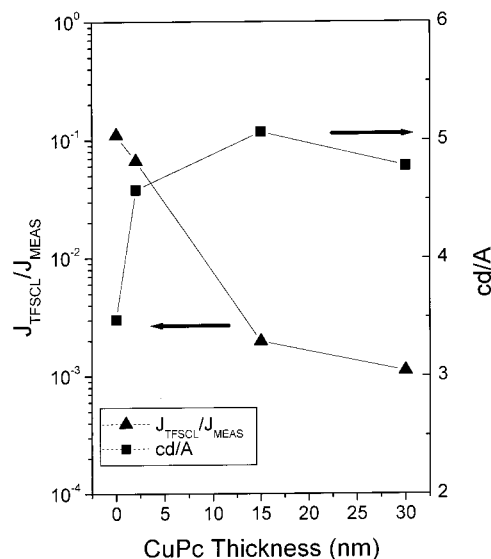


**Figure 5.** Injection efficiency figure of merit,  $J_{\text{meas}}/J_{\text{TFSL}}$  (triangles), for the unipolar TOF devices schematically shown in Figures 3b and 4a as a function of CuPc thickness and at an electric field of  $1.5 \times 10^5$  V/cm. Shown on the same figure is the efficacy, in cd/A (squares), for the bipolar OLEDs schematically shown in Figure 1 as a function of CuPc thickness and at a current density of 42 mA/cm<sup>2</sup>.

precisely this connection, it is interesting to compare the present results with other measurements carried out on similar unipolar hole-transport structures.

The relation between the device performance and the inclusion of a thin layer of CuPc between the ITO substrate and the NPB hole-transporting layer has, in fact, been the subject of several reports from which two alternative models for the role of CuPc on device performance can be inferred.<sup>3–8</sup> On the basis of ultraviolet photoemission spectroscopy (UPS) measurements under ultrahigh vacuum, it was determined that the CuPc HOMO level aligns between the ITO Fermi level and the NPB HOMO levels.<sup>6,7</sup> Further, the UPS data show that the structure of the occupied CuPc molecular orbitals does not change for thicknesses up to 6.5 nm.<sup>6</sup> Such an energy alignment is expected to enhance the hole injection from the ITO substrate into the NPB hole-transporting layer, and this effect was, indeed, manifested in current versus voltage measurements carried out on devices using a 3.5-nm CuPc layer. In contrast, Aziz et al. showed that the 15.0-nm CuPc layer increases the drive voltage, which is thought to improve the carrier balance and, thus, the stability at the emission zone of the OLEDs that they measured.<sup>8</sup>

In the present study, we have examined the efficiency of hole injection from ITO into NPB in devices that incorporate interposed CuPc layers with a thickness range fully overlapping the thicknesses used in all of the previous studies. However, in the present work, the device preparation was fixed, the ITO substrates were commonly sourced, and the NPB transport layers were deposited simultaneously on all four substrates, each overcoated to a different CuPc thickness. It is interesting that the work function of the ITO plates used in the present study was 4.4 eV, essentially identical to that reported in ref 4. Differences in behavior cannot be ascribed to ITO. There remains the possibility that the morphology and the resulting energetics of the deposited CuPc layer are sensitive to the precise details of fabrication. The latter is now the subject of ongoing investigation.

## Summary and Conclusions

A technique that combines TOF drift mobility and dc dark current versus voltage measurements, which are carried out in



the same unipolar trap-free NPB specimen films, has been used to establish an injection efficiency figure of merit for holes supplied from ITO. By this means, we have also established the effect of CuPc layers of varying thickness ranging from 2 to 30 nm, interposed between ITO and NPB, on the efficiency of hole injection from ITO into 5.5- $\mu\text{m}$  NPB films. It is determined that the measured dark current efficiency of injection from the ITO anode into the NPB hole-transporting layer is progressively diminished with increasing CuPc interlayer thickness, starting at a modest 2 nm. At the same time, multilayer bipolar OLED devices exhibit enhanced light output when equally thick CuPc layers are interposed between ITO and the NPB hole-transport medium. These results, which clearly identify a reduced hole injection efficiency with an increase in light output efficacy, lend direct support to the balanced current mechanism described in ref 8.

**Dedication.** Harvey Scher and I (M.A.A.) have been closest friends for nearly our entire lives. Over almost as long a period, we have also shared our academic experiences and then our professional research interests and activities in condensed matter physics. It is a great pleasure to be able to contribute, together with my colleagues, to this dedicatory publication and to offer Harvey my continuing friendship and warmest congratulations.

**Acknowledgment.** This work was supported by DARPA DAAL01-96-K-0086, NSF DMR-9612370, AFOSR 96NL245, and the NSF Center for Photoinduced Charge Transfer. The authors thank Prof. Lewis Rothberg and Dr. Frank Nuesch from

the University of Rochester Chemistry Department for their assistance. Finally, we thank Dr. Ching Tang at the Eastman Kodak Company for his assistance in this work.

## References and Notes

- (1) Tang, C. W.; VanSlyke, S. A. *Appl. Phys. Lett.* **1987**, *51*, 913.
- (2) Tang, C. W.; VanSlyke, S. A.; Chen, C. H. *J. Appl. Phys.* **1989**, *65*, 3610.
- (3) VanSlyke, S. A.; Chen, C. H.; Tang, C. W. *Appl. Phys. Lett.* **1996**, *69*, 2160.
- (4) Kido, J.; Iizumi, Y. *Appl. Phys. Lett.* **1998**, *73*, 2721.
- (5) Hill, I. G.; Kahn, A. *J. Appl. Phys.* **1999**, *86*, 2116.
- (6) Hill, I. G.; Kahn, A. *J. Appl. Phys.* **1998**, *84*, 5583.
- (7) Lee, S. T.; Wang, Y. M.; Hou, X. Y. *Appl. Phys. Lett.* **1999**, *74*, 670.
- (8) Aziz, H.; Popovic, Z. D.; Hu, N. X.; Hor, A. M.; Xu, G. *Science* **1999**, *283*, 1900.
- (9) Abkowitz, M. A.; Pai, D. M. *Philos. Mag. B* **1986**, *53*, 193.
- (10) Abkowitz, M. A.; Facci, J. S.; Stolka, M. *Chem. Phys.* **1993**, *177*, 783.
- (11) Abkowitz, M.; Facci, J. S. *J. Appl. Phys.* **1998**, *83*, 2670.
- (12) Bosenberger, P. M.; Magin, E. H.; Shi, J. *Physica B* **1996**, *217*, 212.
- (13) Forsythe, E. W.; Morton, D. C.; Tang, C. W.; Gao, Y. *Appl. Phys. Lett.* **1998**, *73*, 1457.
- (14) Park, Y.; Choong, V.; Hsieh, B. R.; Tang, C. W. *Appl. Phys. Lett.* **1996**, *68*, 2699.
- (15) Le, Q. T.; Nuesch, F.; Rothberg, L. J.; Forsythe, E. W.; Gao, Y. *Appl. Phys. Lett.* **1999**, *75*, 1357.
- (16) Kim, J. M.; Granstrom, M.; Friend, R. H.; Salaneck, W. R.; Daik, R.; Feast, W. J.; Cacialli, F. *J. Appl. Phys.* **1999**, *84*, 6859.
- (17) Mason, M. G.; Hung, L. S.; Tang, C. W.; Lee, S. T.; Wang, K. W.; Yang, M. *J. Appl. Phys.* **1999**, *86*, 1688.
- (18) Giebeler, C.; Antoniadis, H.; Bradley, D. D. C.; Shirota, Y. *J. Appl. Phys.* **1999**, *85*, 608.